Second random phase approximation studies in metallic clusters

D. Gambacurta[1,2,*] and F. Catara[2,3,†]
[1]*Consortium COMETA, Via S. Sofia 64, I-95123 Catania, Italy*
[2]*Dipartimento di Fisica e Astronomia, Universitá di Catania, Via S. Sofia 64, I-95123 Catania, Italy*
[3]*Istituto Nazionale di Fisica Nucleare, Sezione di Catania, Via S. Sofia 64, I-95123 Catania, Italy*
(Received 5 September 2008; published 3 February 2009)

We study collective states in metallic clusters within the second random phase approximation (RPA) including all kinds of couplings among all one particle–one hole and two particle–two hole configurations. The calculations are done in the jellium approximation. The coupling of one particle–one hole configurations with the two particle–two hole ones strongly pushes down the multipole strength distribution, especially for the dipole case, with respect to RPA. The inclusion of the coupling of the two particle–two hole configurations among themselves enhances this behavior also for the collective states whose description within RPA is widely accepted as satisfactory. Some possible origins of these unpleasant results are discussed. In particular, the need for a better treatment of short-range correlations is underlined.

DOI: 10.1103/PhysRevB.79.085403 PACS number(s): 21.60.Jz, 21.10.Pc, 21.10.Re, 24.30.Cz

I. INTRODUCTION

The random phase approximation (RPA) (Refs. 1 and 2) is widely used as a suitable microscopic theory to study collective modes which can be interpreted in terms of vibrations. In nuclei such vibrations, both low-lying and high-lying [giant resonances (GR)], have been known for a long time.[3] Metallic clusters show the dipole plasmon resonance[4,5] which is the analog of the nuclear dipole GR and is interpreted as due to the collective vibration of the electrons against the positive ions. In both systems, RPA is able to describe the basic properties of these vibrations. However, some limitations are well known. On one hand, RPA predicts a perfectly harmonic spectrum with regularly spaced multiphonon states. Anharmonicities are a well-established phenomenon in nuclei, both experimentally and theoretically.[3,6–11] In metallic clusters no experimental evidence has been found until now for the existence of states corresponding to the double excitation of the dipole plasmon. Theoretically such states have been predicted at energies deviating by about 10% from the double of the plasmon energy.[12,13] Another limitation is that the quasiboson approximation (QBA) is used in deriving the equations of motion of RPA and this introduces a clear loss of self-consistency and violations of the Pauli principle.

A natural extension of RPA is the so-called second RPA (SRPA) (Refs. 14 and 15) where two particle–two hole ($2p-2h$) excitations, in addition to the one particle–one hole ($1p-1h$) ones, are introduced. The derivation of SRPA is also based on QBA and it has been argued[16–18] that in this case its use is even more problematic than in RPA. This point has been recently analyzed in Ref. 19 where an approach to go beyond QBA was presented and applied to a three-level Lipkin model. However, such analysis is limited by the fact that the model is very schematic and contains several parameters. In particular, the relative strengths of the terms of the interaction describing the coupling V_{11} among $1p-1h$ configurations, as well as V_{12} and V_{22}, where 2 indicates the $2p-2h$ configurations, are completely arbitrary. Therefore, one somehow fixes such relative strengths and studies the evolution of the results as a function of an overall interaction strength. By doing so, however, it remains open the question of how much the quality of the agreement with exact results depends on the chosen relative weights.

The aim of the present paper is to analyze merits and limitations of SRPA for the study of the vibrational spectrum of a realistic many-body system. As a test laboratory we have chosen the case of metallic clusters, within the uniform jellium approximation[4,20] with bare Coulomb interaction both for the electrons with the jellium and for the electrons among themselves.[21] The reason for choosing such an admittedly simplified model is that it contains many characteristics of a generic realistic many-body system and the interaction does not contain any adjustable parameter.

We make use of the complete SRPA scheme, including all kinds of coupling within the $1p-1h$ and $2p-2h$ configurations, as they come out from the underlying two-body interaction. To our knowledge, this has never been done before since current versions of SRPA are based on noninteracting $2p-2h$ configurations and only interactions between $2p-2h$ and $1p-1h$ have been explicitly taken into account. Indeed, having in mind to use SRPA as a tool for studying the spreading width of the RPA ("one-phonon") collective states, in the calculations done until now the coupling of the $2p-2h$ configurations among themselves has been completely neglected.[22] As we will see, this approximation does not account fully for the energy shifts of the one-phonon states. In addition to that, of course the study of the spectrum corresponding to double excitations ("two-phonon" states) necessarily requires to take into account those neglected couplings.

In the considered cases, we find a very large shift down of the RPA energies when the $2p-2h$ configurations are included within SRPA. A similar feature has been found also in nuclei.[22]

More general approaches than RPA and SRPA are the so-called time dependent density matrix (TDDM) and second TDDM (STDDM) theories. They have been recently discussed in several works by Tohyama and co-workers.[23–27] They are based on a systematic truncation of the hierarchy of the equations of motion for the one-body and two-body den-

sity matrix. The equations one gets in such a way are more general than the RPA and SRPA ones, the main difference being that many more configurations than $2p-2h$ and $1p-1h$ appear. Indeed, when the correlated ground state is used, rather than the uncorrelated Hartree-Fock (HF) one, configurations of the type pp' and hh' can be build up, in addition to the ph and hp ones considered in RPA. Such an extension of the configuration space has been considered also in Ref. 28 within a three-level Lipkin model. Similarly, many more configurations than in SRPA appear in STDDM. However, the solution of these more general equations would require a tremendous numerical effort if one wants to study a realistic many-body system with a single-particle basis large enough to preserve with a good accuracy, of the order of 1% or less, the energy weighted sum rules. On the other hand, it is certainly instructive to study the limitations of the complete standard SRPA.

The paper is organized as follows. In Sec. II the SRPA framework is presented and its main properties are discussed. In Sec. III we apply it to the study of the excitation spectrum of Na metallic clusters and a comparison with RPA results is carried out. Finally, in Sec. IV, we draw the main conclusions.

II. FORMALISM

In this section we briefly derive the SRPA equations by following the equations of motion method.[1,2] Let $|0\rangle$ be the ground state of the system and $|\nu\rangle$ its excited states whose energies are E_0 and E_ν, respectively. Let us now introduce the operators $Q_\nu^\dagger$ in such a way that

$$Q_\nu^\dagger|0\rangle = |\nu\rangle, \tag{1}$$

$$Q_\nu|0\rangle = 0. \tag{2}$$

It can be shown[2] that the following equations hold for an arbitrary operator δQ:

$$\langle 0|[\delta Q,[H,Q_\nu^\dagger]]|0\rangle = \omega_\nu \langle 0|[\delta Q,Q_\nu^\dagger]|0\rangle, \tag{3}$$

where $\omega_\nu = E_\nu - E_0$ are the excitation energies.

Let $|\mathrm{HF}\rangle$ be the HF ground state of the system where the hole states below the Fermi energy are filled and the particle states above are empty. In the following, we use the indices m, n, p, q and i, j, k, l to indicate, respectively, particle and hole states. In the RPA scheme the $Q_\nu^\dagger$ operators are assumed to be a linear superposition of one particle-hole $(1p-1h)$ operators, that is,

$$Q_\nu^\dagger = \sum_{pi} X_{pi}^\nu a_p^\dagger a_i - \sum_{pi} Y_{pi}^\nu a_i^\dagger a_p, \tag{4}$$

where for notation simplicity, the coupling to total quantum numbers is not indicated. By inserting the above expression in Eq. (3) with $\delta Q \in \{a_p^\dagger a_i, a_i^\dagger a_p\}$ we obtain

$$\begin{pmatrix} A & B \\ -B^* & -A^* \end{pmatrix} \begin{pmatrix} X^\nu \\ Y^\nu \end{pmatrix} = \omega_\nu \begin{pmatrix} X^\nu \\ Y^\nu \end{pmatrix}, \tag{5}$$

where the RPA matrices are

$$A_{pi,qj} = \langle \mathrm{HF}|[a_i^\dagger a_p,(H,a_q^\dagger a_j)]|\mathrm{HF}\rangle, \tag{6}$$

$$B_{pi,qj} = -\langle \mathrm{HF}|[a_i^\dagger a_p,(H,a_j^\dagger a_q)]|\mathrm{HF}\rangle. \tag{7}$$

We stress that the exact ground state $|0\rangle$ has been replaced by the HF ground state $|\mathrm{HF}\rangle$ in the expressions of the RPA matrices (6) and (7). This replacement, also known as QBA, introduces a visible inconsistency since, on one hand, the definition of the ground state $|0\rangle$ as the vacuum of the Q operators is used to derive the formal equations of the motion (3), while, on the other hand, $|\mathrm{HF}\rangle$ is used instead in calculating the expectation values appearing in those equations. Furthermore, the QBA introduces a violation of the Pauli principle since some terms of the double commutators appearing in the equations of motion are missing.

In the SRPA framework, the $Q_\nu^\dagger$ operators have a more general expression, containing also $2p-2h$ terms,

$$Q_\nu^\dagger = \sum_{pi} (X_{pi}^\nu a_p^\dagger a_i - Y_{pi}^\nu a_i^\dagger a_p) + \sum_{p<m,i<j} (X_{pimj}^\nu a_p^\dagger a_i a_m^\dagger a_j - Y_{pimj}^\nu a_i^\dagger a_p a_j^\dagger a_m). \tag{8}$$

In this case we obtain that the X's and Y's are solutions of the equations

$$\begin{pmatrix} \mathcal{A} & \mathcal{B} \\ -\mathcal{B}^* & -\mathcal{A}^* \end{pmatrix} \begin{pmatrix} \mathcal{X}^\nu \\ \mathcal{Y}^\nu \end{pmatrix} = \omega_\nu \begin{pmatrix} \mathcal{X}^\nu \\ \mathcal{Y}^\nu \end{pmatrix}, \tag{9}$$

where

$$\mathcal{A} = \begin{pmatrix} A_{mi,pk} & A_{mi,pqkl} \\ A_{pqkl,mi} & A_{mnij,pqkl} \end{pmatrix},$$

$$\mathcal{B} = \begin{pmatrix} B_{mi,pk} & B_{mi,pqkl} \\ B_{pqkl,mi} & B_{mnij,pqkl} \end{pmatrix},$$

and

$$\mathcal{X}^\nu = \begin{pmatrix} X_{mi}^\nu \\ X_{mnij}^\nu \end{pmatrix}, \quad \mathcal{Y}^\nu = \begin{pmatrix} Y_{mi}^\nu \\ Y_{mnij}^\nu \end{pmatrix}.$$

The elements $A_{mi,pk}$ and $B_{mi,pk}$ of $\mathcal{A}$ and $\mathcal{B}$ are equal to those defined in Eqs. (6) and (7) while the others are

$$A_{mi,pqkl} = \langle \mathrm{HF}|[a_i^\dagger a_m,(H,a_p^\dagger a_q^\dagger a_l a_k)]|\mathrm{HF}\rangle, \tag{10}$$

$$A_{pqkl,mi} = A_{mi,pqkl}^*, \tag{11}$$

$$A_{mnij,pqkl} = \langle \mathrm{HF}|[a_i^\dagger a_j^\dagger a_n a_m,(H,a_p^\dagger a_q^\dagger a_l a_k)]|\mathrm{HF}\rangle, \tag{12}$$

$$B_{mi,pqkl} = -\langle \mathrm{HF}|[a_i^\dagger a_m,(H,a_k^\dagger a_l^\dagger a_q a_p)]|\mathrm{HF}\rangle, \tag{13}$$

$$B_{pqkl,mi} = B_{mi,pqkl}^*, \tag{14}$$

$$B_{mnij,pqkl} = -\langle \mathrm{HF}|[a_i^\dagger a_j^\dagger a_n a_m,(H,a_k^\dagger a_l^\dagger a_q a_p)]|\mathrm{HF}\rangle. \tag{15}$$

Therefore, in SRPA, the QBA is still used. As a consequence of the use of the $|\mathrm{HF}\rangle$ state in the evaluation of the SRPA matrices we obtain, in particular,[14,15]

$$B_{mi,pqkl} = B_{pqkl,mi} = B_{mnij,pqkl} = 0. \tag{16}$$

The matrix (10) describes the coupling of $1p-1h$ states to $2p-2h$ states, while matrix (12) takes into account the coupling between $2p-2h$ states themselves. The dimension of these matrices, especially of the latter, can be very large. If we neglect the residual interaction among the $2p-2h$ states, matrix (12) acquires a simple form,

$$A_{mnij,pqkl} = \mathcal{U}(ij)\mathcal{U}(mn)\delta_{ik}\delta_{jl}\delta_{mp}\delta_{nq}(\epsilon_m + \epsilon_n - \epsilon_i - \epsilon_j), \tag{17}$$

where $\mathcal{U}(ij)$ is the antisymmetrizer for the indices i, j and the ϵ quantities are the HF single-particle energies. In this case, the SRPA problem can be reduced to an RPA eigenvalue problem (5) (whose dimensions are determined by the $1p-1h$ space), but where matrix (6) depends now on the excitation energies ω (Ref. 15).

Let us now recall that, if $|0\rangle$ and $|\nu\rangle$ are a complete set of exact eigenstates of the Hamiltonian, with eigenvalues E_0 and E_ν, the following identity, the so-called energy weighted sum rule (EWSR), holds:

$$\sum_\nu \omega_\nu |\langle \nu|F|0\rangle|^2 = \frac{1}{2}\langle 0|[F,(H,F)]|0\rangle, \tag{18}$$

where $\omega_\nu = E_\nu - E_0$. The above equality is in general violated to some extent when $|0\rangle$, $|\nu\rangle$ and ω_ν are calculated with some approximation. To which extent it is satisfied is a measure of the adequacy of the approximation. We note that the right-hand side is a quantity which depends only on the ground-state properties.

The transition amplitudes $\langle \nu|F|0\rangle$ induced by a one-body operator

$$F = \sum_{\alpha,\beta} \langle \alpha|F|\beta\rangle a_\alpha^\dagger a_\beta \tag{19}$$

between the ground state $|0\rangle$ and excited states $|\nu\rangle$ are

$$\langle \nu|F|0\rangle = \langle 0|[Q_\nu,F]|0\rangle, \tag{20}$$

where definition (1) and the vacuum property (2) have been used. The above expression is general and it is valid independently of the explicit form of the Q operators. In RPA and in SRPA, the above quantity can be calculated by using again the QBA:

$$\begin{aligned}\langle 0|[Q_\nu,F]|0\rangle &\approx \langle \mathrm{HF}|[Q_\nu,F]|\mathrm{HF}\rangle \\ &= \sum_{ph} \{X_{ph}^{\nu *}\langle p|F|h\rangle + Y_{ph}^{\nu *}\langle h|F|p\rangle\}.\end{aligned} \tag{21}$$

Thus, the use of the QBA has two important consequences. For what concerns the transition operator, we observe that only its $p-h$ components are selected. Furthermore, we note that, also in the case of the SRPA, only the $1p-1h$ amplitudes appear in the above equation.

A very important feature of RPA and SRPA, known as Thouless theorem,[29] can be described as follows. When the left-hand side of Eq. (18) is evaluated by using the energies and the X and Y amplitudes of RPA (SRPA), one finds the same result as when the right-hand side of the same equation is calculated by replacing the exact ground $|0\rangle$ with the $|\mathrm{HF}\rangle$ state. Thus, the first moment

$$m_1 = \sum_\nu \omega_\nu |\langle \nu|F|0\rangle|^2 \tag{22}$$

is the same in RPA and SRPA.[15,30]

Finally we recall that, if F is a multipole operator $r^L Y_{L0}$ and the Hamiltonian contains a kinetic energy term plus a local two-body interaction, the right-hand side of Eq. (18) is[2]

$$\frac{1}{2}\langle 0|[F,(H,F)]|0\rangle = \frac{\hbar^2}{2m}\frac{L(2L+1)}{4\pi}N\langle 0|r^{2L-2}|0\rangle, \tag{23}$$

N being the number of particles and

$$\langle 0|r^{2L-2}|0\rangle = \frac{1}{N}\sum_{\alpha,\beta}\rho(\alpha,\beta)\int r^{2L-2}\varphi_\alpha(r)\varphi_\beta^*(r)r^2dr, \tag{24}$$

where α and β stand for any single-particle states with wave functions $\varphi_\alpha(r)$ and $\varphi_\beta(r)$. Of course, when the ground state is described by the HF one, Eq. (24) becomes

$$\langle \mathrm{HF}|r^{2L-2}|\mathrm{HF}\rangle = \frac{1}{N}\sum_h \int r^{2L-2}|\varphi_h(r)|^2 r^2 dr. \tag{25}$$

III. RESULTS

In the present paper we remain at the standard SRPA level of approximation but we exploit all its potentiality by performing full calculations, including all kinds of couplings among all configurations, for a realistic many-body system. In order to analyze merits and limitations of SRPA, we have chosen to apply it to the study of metallic clusters within the jellium approximation. The reason for this choice is that the interaction of the electrons among themselves and with the ionic background is completely fixed as the bare Coulomb interaction and the model does not contain any adjustable parameter. This allows to compare in a clear way different degrees of approximation.

The Hamiltonian of the system is

$$H = \sum_i h_i + \sum_{i<j} v_{ij}, \tag{26}$$

with

$$h_i = -\frac{\hbar^2}{2m}\nabla_i^2 + V(r_i), \quad v_{ij} = \frac{e^2}{4\pi}\frac{1}{|\vec{r}_i - \vec{r}_j|}, \tag{27}$$

and

$$V(r) = \frac{Ne^2}{4\pi}\begin{cases}(1/2r_c)(r^2/r_c^2 - 3) & \text{for } r \le r_c \\ -1/r & \text{for } r \ge r_c,\end{cases} \tag{28}$$

where r_c is the radius of the jellium sphere, i.e., $r_c = r_s N^{1/3}$, r_s being the Wigner-Seitz radius and N the number of ions.

As a first step, we have fixed, by solving the HF equations, the single-particle basis in which all the subsequent calculations are carried out. The single-particle wave functions have been represented as linear superposition of har-

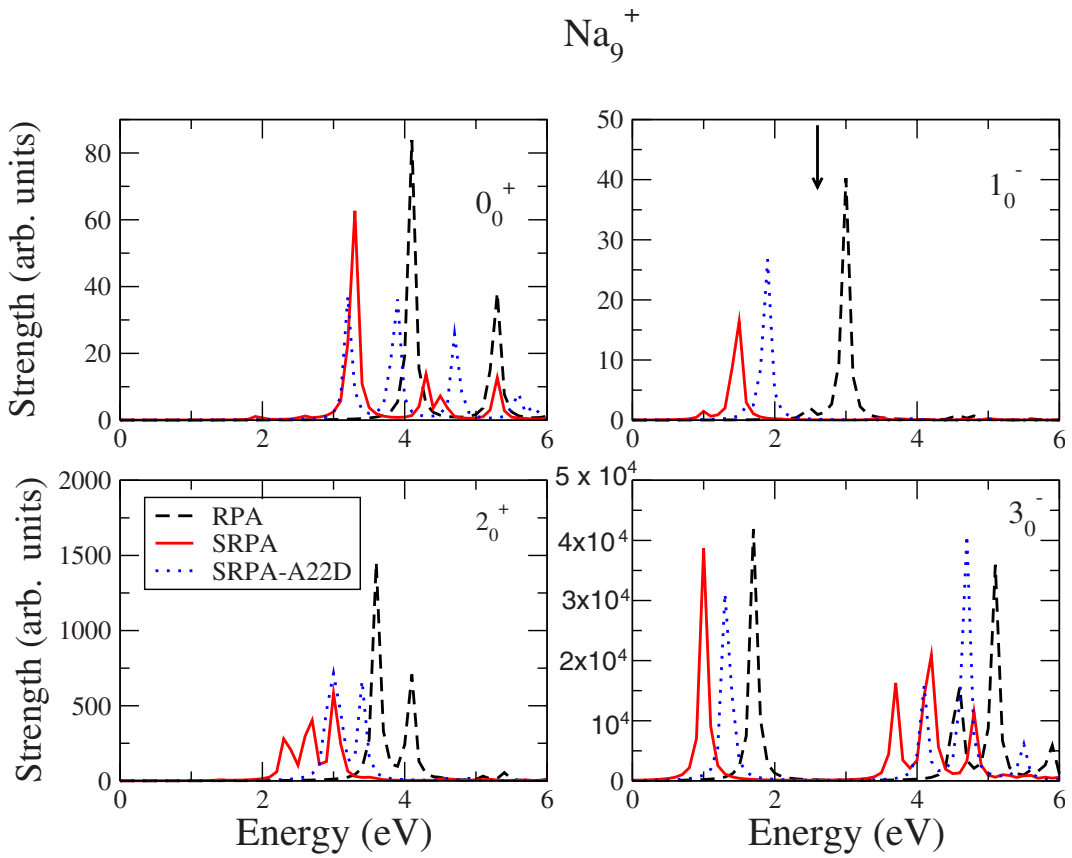

FIG. 1. (Color online) Natural parity $L=0,1$ (upper panel) and $L=2,3$ (lower panel) spin=0 multipole strength distributions for Na_9^+ metallic cluster are shown. Solid (red) lines refer to SRPA results, while the dashed (black) ones refer to RPA calculations. SRPA-A22D dotted (blue) lines show the SRPA results when the approximation (17) is used. The arrow roughly indicates the positions of the experimental dipole plasmon peak.

monic oscillator ones, with principal quantum number ranging from $n=0$ to $n=35$ for each orbital angular momentum l. After that, we have solved the RPA and SRPA equations for natural parity states, with multipolarities ranging from $L=0$ to $L=3$. The single-particle space has been truncated so that the Thouless theorem, and thus the preservation of EWSR, is satisfied in the RPA calculations better than 1% for all the multipolarities. We focus our attention only on spin $S=0$ states. However we remark that, for what concerns the SRPA calculations, all the $1p-1h$ states with $L=0-3$, both spin $S=0$ and 1, are considered in the construction of the $2p-2h$ configurations with good total spin and angular momentum.

In the following we show the results for two sodium clusters, namely, the Na_9^+ and Na_{21}^+. In the latter case an energy cutoff E_{cut} has been used and only the $2p-2h$ configurations with unperturbed energy lower than $E_{cut}=15$ eV are included. In order to check whether the single-particle spaces used in the two calculations are large enough to give stable results we show in Tables I and II the values of the right-hand side (rhs) of Eq. (18) calculated in the HF state and, correspondingly, the left-hand side (lhs) calculated in RPA and SRPA for the multipole operator,

$$F^{(L)}(r) = r^L Y_{L0}. \tag{29}$$

In Table I, for the Na_9^+ case, we see that the EWSR is satisfied better than 1% for all the multipolarities. As expected, the values of lhs calculated in RPA and SRPA are the same, since, as mentioned above, the first moment (22) is the

TABLE I. The values of the rhs of Eq. (18), in units of $Å^{2L}$ eV, calculated in the HF state and, correspondingly, the lhs calculated in RPA and SRPA in the case of Na_9^+ for the different multipolarities L. Results refer to the multipole operator (29).

	rhs	lhs in RPA	lhs in SRPA
$L=0$	0.11541×10^3	0.11558×10^3	0.11558×10^3
$L=1$	0.21901×10^2	0.21909×10^2	0.21909×10^2
$L=2$	0.14426×10^4	0.14446×10^4	0.14446×10^4
$L=3$	0.70494×10^5	0.70414×10^5	0.70414×10^5

TABLE II. As in Table I but for Na_{21}^+ metallic cluster. The SRPA calculations have been carried out by including all the $2p-2h$ configurations with unperturbed energy lower than $E_{cut}=15$ eV.

	rhs	lhs in RPA	lhs in SRPA
$L=0$	0.51514×10^3	0.51459×10^3	0.51033×10^3
$L=1$	0.54755×10^2	0.54733×10^2	0.54167×10^2
$L=2$	0.64392×10^4	0.64299×10^4	0.64193×10^4
$L=3$	0.52823×10^6	0.52478×10^6	0.52285×10^6

same in both the approximations. Similar results are found in the Na_{21}^+ case shown in Table II. In this case, since an energy cutoff E_{cut} for the $2p-2h$ configurations has been used, the values of lhs calculated in RPA and SRPA are slightly different. However, in the worst case, namely for $L=1$, the discrepancy is of the order of 1% and therefore we can conclude that the truncated $2p-2h$ space is large enough.

In Fig. 1 we plot the strength distributions for the multipole operator $F^{(L)}$ [Eq. (29)] for the Na_9^+ metallic cluster. In order to make clearer the comparison, the discrete lines of RPA and SRPA spectra are folded with a Lorentzian function. In both cases an artificial width $\Gamma=0.1$ eV has been used. In the upper and lower panel of Fig. 1, we show, respectively, the $L=0,1$ and $L=2,3$ multipole strength distributions with spin $S=0$ for Na_9^+ metallic cluster. Solid (red) lines refer to SRPA results, while the dashed (black) ones refer to those obtained within RPA. With the dotted (blue) lines we indicate the SRPA results when the diagonal approximation (17) is used. In the following figures we use the label "SRPA-A22D" for the results obtained when this diagonal approximation is used.

We see that going from RPA to SRPA the strength distributions are shifted to lower energies, especially in the dipole case. The results shown in Fig. 1 refer to the lower part of the excitation spectrum, which is mainly composed by $1p-1h$ configurations. However, even for such states the inclusion of the coupling among $2p-2h$ configurations leads to a further shift down. Let us look in some detail to the collective dipole $S=0$ state, which in RPA is located at 2.98 eV, and that experimentally is found at about 2.60 eV (Ref. 31). Within the approximated SRPA, that is when only the coupling of $1p-1h$ to $2p-2h$ configurations is taken into account, the energy moves to 1.88 eV, while in the full SRPA one gets 1.47 eV. Furthermore the fraction of EWSR exhausted by this state goes from 88% to 25%. This effect is caused from one hand by the energy shift and, on the other hand, is connected to the reduction in the transition probability [i.e., the square modulus of Eq. (20)] that goes from the RPA value of 6.48 $Å^2$ to 3.74 $Å^2$ in SRPA.

It is also instructive to look into the structure of the wave functions in the two cases. Remembering the SRPA normalization condition,

$$\sum_{pi}(|X_{pi}^{\nu}|^2-|Y_{pi}^{\nu}|^2)+\sum_{p<m,i<j}(|X_{pimj}^{\nu}|^2-|Y_{pimj}^{\nu}|^2) = N^{(1)}+N^{(2)}=1, \tag{30}$$

we have calculated the $N^{(1)}$ and $N^{(2)}$ quantities, which give an indication of the $1p-1h$ and $2p-2h$ content in the state. For the collective plasmon state, $N^{(2)}$ turns out to be 8% within the approximate SRPA and it goes up to 16% in the full calculation. Thus we see that, the parts of the residual interaction coupling the $2p-2h$ configurations among themselves strongly affect both the energy and the wave function, even for a state whose nature is mainly of $1p-1h$ character.

In all the cases, the SRPA strength distributions are shifted to lower energies with respect to the RPA ones, and, at the same time, the height of the main peaks is reduced. However, as discussed in Sec. II, the first moment m_1 [Eq. (22)] is the same in RPA and SRPA (see Table I). In fact, although the high-lying SRPA states have a small probability to be excited by the transition operator (having them a strong $2p-2h$ nature), their overall contribution to m_1 is quite big. For example, in the dipole case, the states lying above 10 eV exhaust 40% of m_1. In order to make clearer this effect, we plot in Fig. 2 the same dipole strength distribution shown in Fig. 1, but using a logarithmic ordinate scale and a wider range for the excitation energy in abscissa. In the same figure we see that, as expected, the coupling of $2p-2h$ configurations among themselves strongly modifies the strength distribution in the higher part of the excitation spectrum.

As shown in Fig. 3, qualitatively similar results have been found for Na_{21}^+. Also in this case we have a strong shift down, especially for the dipole excitations, the plasmon energy being lowered from the RPA value of 2.90 eV to the full SRPA result of 1.00 eV very far from the experimental peak at about 2.65 eV.[31] Again, very striking is the fact that the fraction of EWSR exhausted by this state goes from 79% to 10%, while the total m_1, Eq. (22), is quite the same of the RPA value (see Table II). In Fig. 4, where we show the evolution of the SRPA strength increasing the energy cutoff E_{cut} for the $2p-2h$ configurations in the dipole case, we see that a good convergence has been reached. Similar results have been obtained for the other multipolarities.

In order to have a deeper insight on these results, we have considered the limiting case of a highly positively ionized Na cluster. Of course, such a cluster cannot exist because of the strong repulsion among the ions. What makes it very interesting from the theoretical point of view is that the intense attraction makes the electrons very well confined in the most interior part of the jellium, $r \ll r_c$ [see Eq. (28)], and their interaction with the positive background behaves as a harmonic oscillator well,

$$V(r)=\text{const}+\frac{1}{2}m_e(\omega_{\text{Mie}}r)^2, \tag{31}$$

where m_e is the electron mass and ω_{Mie} is the Mie frequency. Thus, in this limiting case, the center of mass motion of the

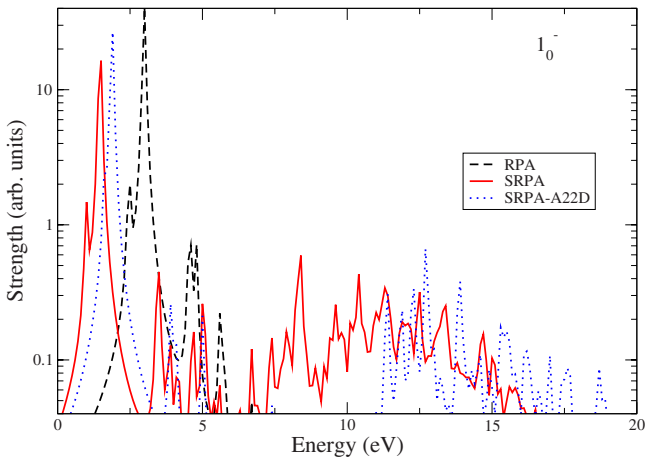

FIG. 2. (Color online) Spin=0 dipole strength for Na_9^+ metallic cluster. Solid (red) lines refer to SRPA results, while the dashed (black) ones refer to RPA calculations. SRPA-A22D dotted (blue) line shows the SRPA results when the approximation (17) is used.

TABLE III. The sum of the squares of the Y^{ν}_{ph} amplitudes in the case of Na_9^+ and for different multipolarities, in RPA (first column), in SRPA (third column), and in SRPA when the diagonal approximation (17) is used (second column).

	$\Sigma_{ph,\nu}\|Y^{\nu}_{ph}\|^2$		
	RPA	SRPA-A22D	SRPA (full)
$L=0$, $S=0$	0.0458	0.0512	0.0532
$L=1$, $S=0$	0.1601	0.2962	0.4170
$L=2$, $S=0$	0.0256	0.0316	0.0347
$L=3$, $S=0$	0.0198	0.0282	0.0388

TABLE IV. The largest $\|Y^{\nu}_{ph}\|^2$ for the case of Na_9^+, in RPA (first column), in SRPA (third column), and in SRPA when the diagonal approximation (17) is used (second column).

	Largest $\|Y^{\nu}_{ph}\|^2$		
	RPA	SRPA-A22D	SRPA (full)
$L=0$, $S=0$	0.0026	0.0031	0.0039
$L=1$, $S=0$	0.0978	0.1429	0.1836
$L=2$, $S=0$	0.0033	0.0042	0.0042
$L=3$, $S=0$	0.0129	0.0203	0.0298

electrons separates exactly and the dipole response is a single line, at an energy $\hbar\omega_{\mathrm{Mie}}=3.4$ eV for Na clusters, having 100% EWSR. These expectations are very well confirmed within RPA.[32] We have checked again numerically this for the case of the eightfold positive ionized Na_{16}^{8+} cluster and have found the dipole strength being strongly concentrated (99.93% of the EWSR) at $E=3.38$ eV. This very nice picture is completely spoiled when we go to SRPA: the main peak is moved down to 1.50 eV and it exhausts only the 70% of the EWSR. Therefore we can conclude that SRPA is not doing a good job and its results are definitely worse than RPA. This problem would not arise if one takes into account the complete space of all kinds of configurations of the STDDM approach.[23] This is however well beyond the scopes of the present paper and it should require to handle matrices of very large dimensions. As mentioned above, in our calculations the bare Coulomb interaction between the electrons and the jellium as well as among the electrons is used. Although we are aware that more realistic approaches should be used[33,34] in order to describe properly possible screening effects, a qualitative idea on how much the difficulties of SRPA are due to the use of the bare interaction can be obtained by using a Yukawa-type interaction

$$V_0\frac{e^{-\mu r}}{r}, \tag{32}$$

with V_0 fixed, for each μ, in such a way that

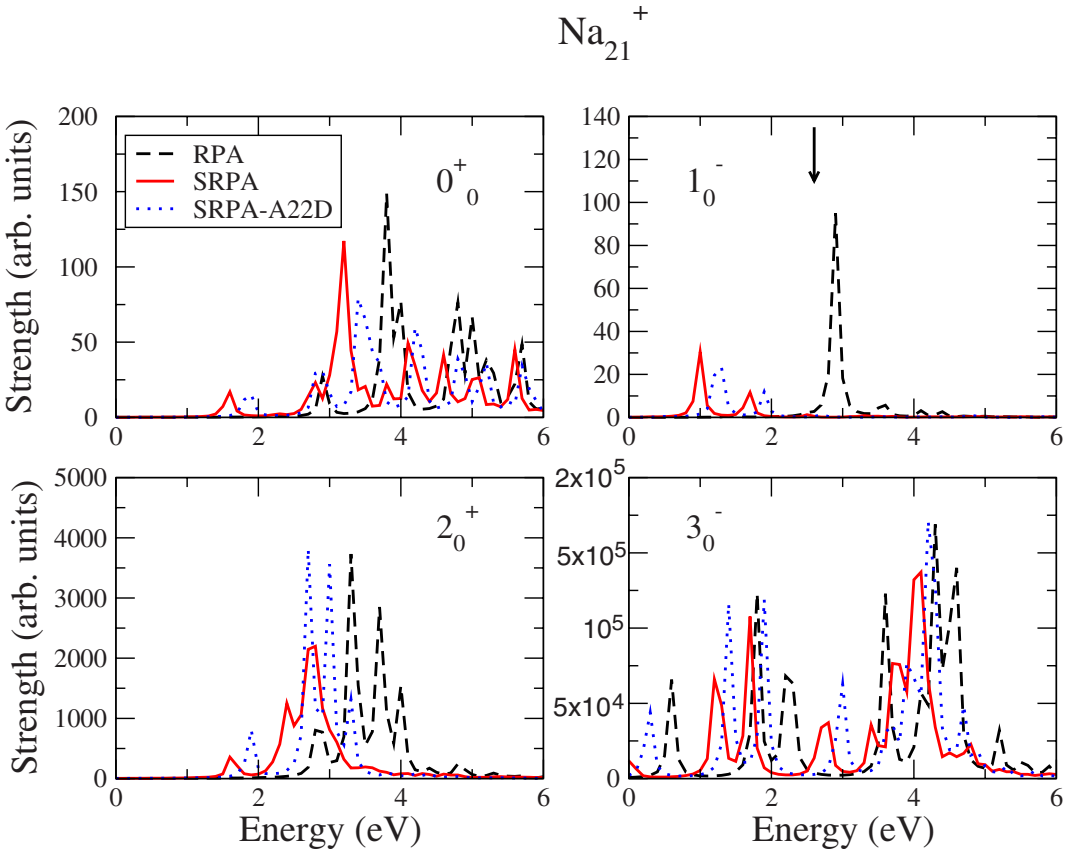

FIG. 3. (Color online) As in Fig. 1 but for Na_{21}^+ metallic cluster.

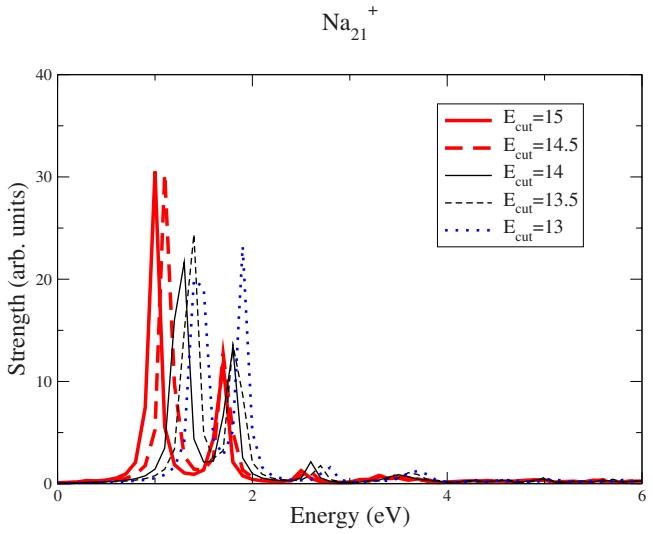

FIG. 4. (Color online) Dipole SRPA strength as a function of the energy cutoff $E_{\rm cut}$, ranging from 13 eV to 15 eV, for the $2p-2h$ configurations.

$$e^2\int_0^{r_c} r^2\frac{1}{r}dr = e^2V_0\int_0^{r_c} r^2\frac{e^{-\mu r}}{r}dr. \tag{33}$$

However, the comparison between RPA and SRPA results is qualitatively the same as with the bare Coulomb interaction. On the other hand, also in the nuclear[22] case one finds that the SRPA excitation spectrum is very much different from the RPA one, even for excitations like the giant resonances whose description within RPA is widely accepted as satisfactory. Probably in all cases, the problems arise from the fact that the self-energy-like terms present in SRPA take contributions from very high energy "incoherent" particle-hole configurations. Indeed, such disturbing features do not appear when the extension of RPA is made by coupling particle-hole configurations with collective phonons.[35–37] In addition to that, we stress again that the derivation of the SRPA equations of motion is based on QBA and this might be more doubtful than in RPA. Indeed, a better treatment of ground-state correlations has been found to improve the results, within a three-level Lipkin model.[19] As discussed above, in order to derive the equations of motion, both in RPA and SRPA, use is made of the QBA. However, the replacement of the correlated ground state with the HF one is justified only if ground-state correlations are not too strong. In RPA the Y^ν_{ph} amplitudes are a measure of these correlations[2] and thus, looking at their behavior going from RPA to SRPA could be useful in order to have more information about the adequacy of QBA. In Table III we report, in the case of Na_9^+ and for different multipolarities, the sum of the squares of the Y^ν_{ph} amplitudes in RPA (first column), in SRPA (third column), and in SRPA when the diagonal approximation (17) is used (second column). We see that going from RPA to SRPA an increase of these quantities is observed and the inclusion of the residual interaction coupling the $2p-2h$ configurations among themselves amplifies this effect. The same behavior is found for the largest $|Y^\nu_{ph}|^2$ shown in Table IV and it is especially strong, as for the shift of the strength distribution, in the dipole case. A similar analysis has been done in the case of Na_{21}^+; see Tables V and VI, where even larger enhancements of the Y^ν_{ph} are indeed observed.

TABLE V. As in Table III but for the Na_{21}^+ case.

	$\Sigma_{ph,\nu}\|Y^\nu_{ph}\|^2$		
	RPA	SRPA-A22D	SRPA (full)
$L=0$, $S=0$	0.1031	0.1100	0.0926
$L=1$, $S=0$	0.3325	0.9465	1.3200
$L=2$, $S=0$	0.0879	0.1082	0.1112
$L=3$, $S=0$	0.0866	0.1080	0.1606

Although both in RPA and SRPA the $|\mathrm{HF}\rangle$ state is used in evaluating the matrices appearing in the equations of motion, in RPA, the form of the ground state, defined as the vacuum of the Q operators, can be explicitly obtained[2] within the quasiboson approximation. It has the form

$$|\mathrm{RPA}\rangle \propto e^{\hat{Z}}|\mathrm{HF}\rangle, \tag{34}$$

with

$$\hat{Z} = \frac{1}{2}\sum_{p_1h_1p_2h_2} Z_{p_1h_1p_2h_2}a^\dagger_{p_1}a_{h_1}a^\dagger_{p_2}a_{h_2}, \tag{35}$$

where the Z matrix satisfies the following relation:

$$Z = Y^*X^{*^{-1}}. \tag{36}$$

The RPA occupation numbers can be calculated by using, for example, the number operator method[38] and one gets

$$n_h = 1 - \frac{1}{2}\sum_{p,\nu}|Y^\nu_{ph}|^2, \tag{37}$$

and

$$n_p = \frac{1}{2}\sum_{h,\nu}|Y^\nu_{ph}|^2. \tag{38}$$

We remark that the above expressions for the occupation numbers differ from those obtained by making use of the QBA by the factor $\frac{1}{2}$. The same result was obtained in Ref. 39. To our knowledge, the explicit form of the correlated SRPA ground state has not been obtained, as well as an ex-

TABLE VI. As in Table IV but for the Na_{21}^+ case.

	Largest $\|Y^\nu_{ph}\|^2$		
	RPA	SRPA-A22D	SRPA (full)
$L=0$, $S=0$	0.0026	0.0036	0.0031
$L=1$, $S=0$	0.1388	0.5423	0.6861
$L=2$, $S=0$	0.0059	0.0106	0.0067
$L=3$, $S=0$	0.0199	0.0263	0.0452

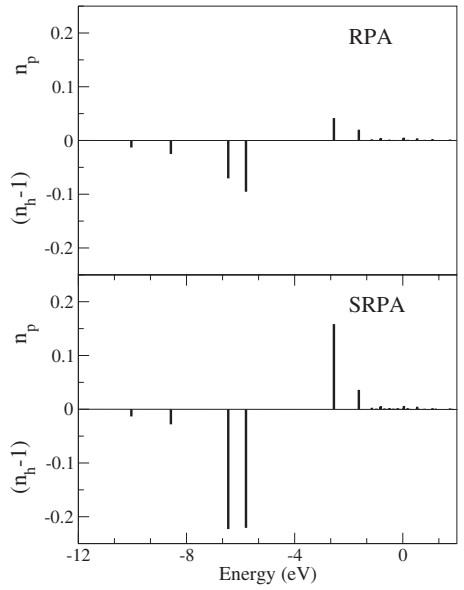

FIG. 5. Occupation numbers n_p for particle states and the opposite of depletion numbers n_h-1 for hole states for Na_{21}^+ metallic cluster. RPA and SRPA results are reported in the upper and lower panel, respectively. Only spin $S=0$ states are included in the calculations. In the abscissa the single-particle energies in eV are indicated.

pression for the SRPA occupation numbers. Nevertheless, it could be instructive to compare the values of quantities (37) and (38) when the Y_{ph}^{ν} obtained in RPA and SRPA are used. In this sense we will refer in the following to SRPA occupation numbers.

In Fig. 5 we show, in the case of the Na_{21}^+ metallic cluster, the occupation numbers n_p for particle states and the opposite of the depletion numbers n_h-1 for hole states obtained in SRPA and in RPA, in the lower and upper panel, respectively. All states with $L=0-3$ and spin $S=0$ are used in the calculation of these quantities. We note that the deviations from the HF limit, i.e., $n_h=1$ and $n_p=0$, are greater in SRPA than in RPA. Since, as mentioned above, the use of QBA is justified only when the HF state does not differ very much from the correlated one, the larger deviations found in SRPA suggest that this approximation could be more severe than in RPA.

As discussed at end of Sec. II, the SRPA problem can be reduced to an energy-dependent RPA problem. In this case, the new RPA $\tilde{A}$ matrix is

$$\tilde{A}_{1,1'}(\omega) = A_{1,1'} + _{1,1'}(\omega), \tag{39}$$

where A is the usual RPA matrix, Σ is the energy-dependent term

$$\Sigma_{1,1'}(\omega) = \sum_{2,2'} A_{1,2}(\omega + i\eta - A_{2,2'})^{-1} A_{2',1'}, \tag{40}$$

and the indices 1 and 2 are a short-hand notation for the $1p-1h$ and $2p-2h$ configurations, respectively. The energy-dependent term is connected to the self-energy of the $1p-1h$ excitation and it is due to the coupling with the $2p-2h$ configurations. It has been shown that its real part gives a shift of the RPA resonance energies while the imaginary part takes into account spreading width effects.[40–42] Several SRPA calculations have been done by neglecting the real part of the particle-hole self-energy (see for example Refs. 15 and 43) and considering only the spreading width. The justification of this choice is based on the fact that, when effective interactions are used, self-energy contributions are already taken into account in the single-particle energies. Thus, in order to avoid double counting, the real part of the particle-hole self-energy is omitted. However, since the real and imaginary part of the self-energy obey a dispersion relation,[41] a consistent treatment of both contributions should be necessary. Furthermore, in our calculations the bare Coulomb interaction is used and no double counting occurs. So it is interesting to study the energy shift due to the real part of the self-energy in this case. In order to have a quantitative, though approximate, evaluation of this effect we consider the self-energy acquired by a RPA phonon as a consequence of the coupling with the $2p-2h$ configurations,[42]

$$\Sigma^{\mathrm{RPA}}(\omega_\nu) = \sum_{2p2h} \frac{|\langle \nu|V|2p2h\rangle|^2}{\omega_\nu - \epsilon_{2p2h} + i\eta}, \tag{41}$$

where ω_ν is the excitation energy of the RPA phonon $|\nu\rangle$, V is the residual interaction, and ϵ_{2p2h} is the unperturbed energy of the $2p-2h$ configuration $|2p2h\rangle = a_{p_2}^\dagger a_{h_2} a_{p_1}^\dagger a_{h_1}|\mathrm{HF}\rangle$. We have calculated the real part of this quantity for the dipole plasmon in the Na_9^+ case. The η parameter used in the calculation is 0.2 eV. As above mentioned, the RPA dipole plasmon ω_ν is located at 2.98 eV. Since the unperturbed $2p-2h$ energies ϵ_{2p2h} are larger than this value, the denominator in Eq. (41) is always negative and thus the resonance peak is shifted downward with respect to ω_ν. In the upper panel of Fig. 6 we plot the absolute value of the real part of the RPA self-energy as a function of a cutoff energy E_c on the $2p-2h$ configurations, i.e., only the $2p-2h$ configurations with unperturbed energy lower than E_c are considered in Eq. (41). We see that increasing the cutoff E_c the energy shift increases until it reaches a saturation value of about 1.5 eV. We remark that this shift is consistent with the one obtained in the SRPA calculation (see Fig. 1). In order to have a deeper insight, we show in the medium panel of Fig. 6 the absolute value of the real part of the quantities

$$k(\epsilon_{2p2h}) = \frac{|\langle \nu|V|2p2h\rangle|^2}{\omega_\nu - \epsilon_{2p2h} + i\eta}, \tag{42}$$

i.e., the contribution to the self-energy of each $2p-2h$ configuration identified by its unperturbed energy ϵ_{2p2h}. We see that, although the largest contributions are given by the lower $2p-2h$ configurations, also the ones with higher energy contribute and the overall effect is quite large. In order to put in evidence in a clearer way this fact, we have divided the unperturbed $2p-2h$ energy range in bins of 0.5 eV and we have summed all the terms defined in Eq. (42) lying in each interval identified by the index I. In the lower panel of Fig. 6, where we plot the absolute value of the real part of the quantities

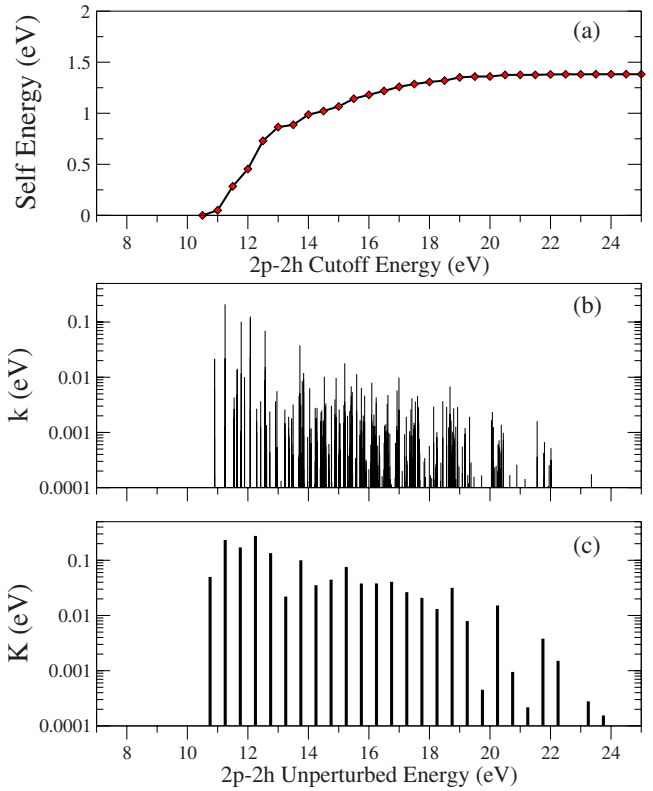

FIG. 6. (Color online) Panel (a): The absolute value of the real part of the RPA self-energy defined in Eq. (41) as a function of the cutoff energy of the $2p-2h$ configurations. Panels (b) and (c): The absolute value of the real part of the k and K quantities defined in Eqs. (42) and (43), respectively. The abscissa of both the figures shows the unperturbed energies of the $2p-2h$ configurations.

$$K(I) = \sum_{\epsilon_{2p2h} \in I} k(\epsilon_{2p2h}), \tag{43}$$

we see that the total contributions of high energy configurations, arising from a coherent sum of many small terms, become comparable with the ones of the lowest energies. Similar results are obtained in the case of Na_{21}^{+}.

Above, we have discussed and analyzed two possible reasons why SRPA strongly modifies RPA results, i.e., effects due to the QBA and to the self-energy of the particle-hole excitations. In QBA the uncorrelated HF state, in place of the correlated one, is used in the calculation of the matrix elements appearing in the equations of motion. Overcoming QBA means taking into account ground-state correlations, if possible in a self-consistent way (see for example Refs. 19, 25, 27, and 44–46 and references therein). By the above-shown analysis of the Y amplitudes and of the occupation numbers, we can conclude that a better treatment of these correlations should be necessary, going beyond standard SRPA. In order to evaluate the effect of the inclusion of ground-state correlations, we have calculated the RPA self-energy defined in Eq. (41) by using the state[15]

$$|0\rangle = \frac{1}{M}\left(|\mathrm{HF}\rangle + \sum_{p_2h_2p_1h_1} C_{p_2h_2p_1h_1} a^{\dagger}_{p_2} a_{h_2} a^{\dagger}_{p_1} a_{h_1} |\mathrm{HF}\rangle\right), \tag{44}$$

where the coefficients are evaluated in first order Rayleigh-Schrödinger perturbation theory, i.e.,

$$C_{p_2h_2p_1h_1} = \frac{\langle \mathrm{HF}| V a^{\dagger}_{p_2} a_{h_2} a^{\dagger}_{p_1} a_{h_1} |\mathrm{HF}\rangle}{\epsilon_{2p2h}}, \tag{45}$$

where ϵ_{2p2h} are the unperturbed energies of the $2p-2h$ excitations and V is the residual interaction. The results are shown in the right panels of Fig. 7, where we plot, in the upper panel, the absolute value of the real part of the RPA self-energy while in the lower one the quantities defined in Eq. (43). For comparison we show in the left panels the corresponding results when the uncorrelated HF state is used and that we have discussed in details in Fig. 6. Please note that, differently from the panel (c) of Fig. 6, a linear ordinate scale is used in order to have a clearer comparison. By comparing the upper panels, we see that when the correlated ground state (44) is used the real part of the self-energy, and thus the energy shift, decreases, the effect being of about 30%. The lower panels show that this decreasing is related to a reduction in the cumulative contributions K. When the HF state is used, the energy shift is 1.38 eV and the total contribution of the $2p-2h$ configurations lying below 13 eV is 0.86 eV, while, when ground-state correlations are included, these values become 0.93 eV and 0.57 eV, respectively. So both low and high energy contributions are lowered by about 30%.

IV. CONCLUSIONS

In the present paper we have found that within SRPA one gets very strong modifications of the RPA excitation spectrum of metallic clusters, the energy being pushed down. When the coupling of $2p-2h$ configurations among themselves is included, a further lowering is obtained even for those collective excitations whose description within RPA is widely assumed as satisfactory. Among the reasons for such a behavior, which would completely spoil some nice properties of RPA, we have discussed two aspects:

(1) the use of QBA in calculating the expectation values appearing in the equations of motion of SRPA. Although the same approximation is used in RPA, it seems more severe in SRPA. As found in Ref. 19 within a Lipkin model, a better treatment of correlations in the ground state leads to important corrections in the energy spectrum.

(2) The $2p-2h$ configurations included in SRPA introduce self-energy corrections[40–43,47] and their contributions are quite large when the uncorrelated HF reference state is used in calculating the A and B matrices.

Very similar results have been obtained by calculating the real part of the self-energy acquired by the RPA collective dipole plasmon through its coupling to $2p-2h$ configurations. In order to estimate how important would be to go beyond QBA, we have calculated the same quantity by including ground-state correlations perturbatively and we have

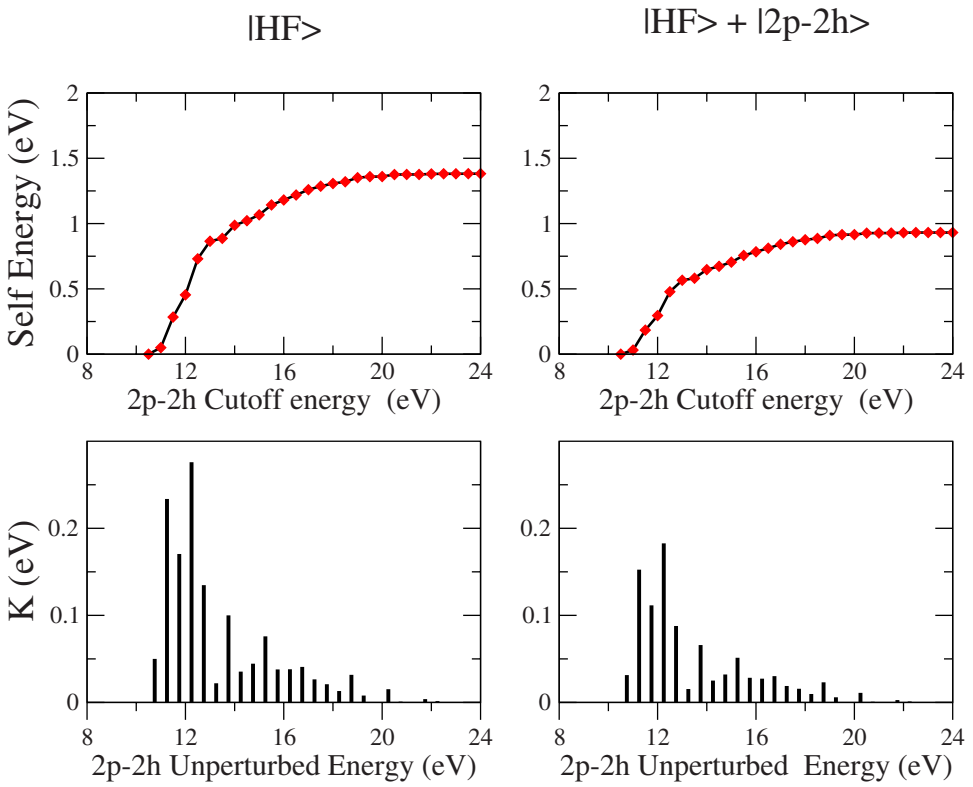

FIG. 7. (Color online) In the upper panels we plot the absolute value of the real part of the RPA self-energy [Eq. (41)] as a function of the cutoff energy of the $2p-2h$ configurations. In the lower panels the absolute values of the real part of the quantities defined in Eq. (43) as functions of unperturbed energies of the $2p-2h$ configurations are shown. In the left panels we show the results obtained by using the uncorrelated HF state while in the right ones the corresponding quantities calculated with the correlated state (44).

found an appreciable reduction in the energy shift.

These results suggest that a better treatment of ground-state correlations along the path of extended RPA and SRPA approaches, as done for example in Refs. 19 and 46, is necessary. Work in this direction is in progress.

The SRPA results could also be related to the fact that short-range correlations are neglected in our description. In this respect, it should be interesting to test whether the use of effective interactions, derived from density functional and including such short-range correlations, can improve SRPA description. Maybe the very strong shift down of the giant resonances obtained in Ref. 22 when passing from RPA to SRPA in ^{16}O and ^{40}Ca nuclei has similar origin if the short-range correlations included in the bare Argonne V18 potential with the unitary correlation operator method, up to two-body terms, are not sufficient.

It is also interesting to analyze how much such strong modifications with respect to RPA description depend on the studied system. In this respect, in the near future, we plan to apply SRPA in nuclear systems by using effective Skyrme-type interactions.

ACKNOWLEDGMENTS

The authors gratefully thank M. Sambataro for helpful discussions and reading the paper. This work makes use of results produced by the PI2S2 Project managed by the Consorzio COMETA, a project cofunded by the Italian Ministry of University and Research (MIUR) within the Piano Operativo Nazionale Ricerca Scientifica, Sviluppo Tecnologico, Alta Formazione (PON 2000–2006). More information is available at http://www.pi2s2.it and http://www.consorzio-cometa.it.

*Danilo.Gambacurta@ct.infn.it
†Francesco.Catara@ct.infn.it

[1] D. J. Rowe, *Nuclear Collective Motion* (Methuen, London, 1970).
[2] P. Ring and P. Schuck, *The Nuclear Many-Body Problem* (Springer-Verlag, Berlin, 1980).
[3] A. Bohr and B. R. Mottelson, *Nuclear Structure* (Benjamin, New York, 1975), Vol. II.
[4] M. Brack, Rev. Mod. Phys. **65**, 677 (1993).
[5] W. A. de Heer, Rev. Mod. Phys. **65**, 611 (1993).
[6] Ph. Chomaz and N. Frascaria, Phys. Rep. **252**, 275 (1995).
[7] M. N. Harakeh and A. van der Woude, *Giant Resonances* (Clar-

endon, Oxford, 2001).
[8] J. de Boer, R. G. Stokstad, G. D. Symons, and A. Winther, Phys. Rev. Lett. **14**, 564 (1965).
[9] C. Volpe, F. Catara, P. Chomaz, M. V. Andresand, and E. G. Lanza, Nucl. Phys. A. **589**, 521 (1995).
[10] E. G. Lanza, M. V. Andrés, F. Catara, Ph. Chomaz, and C. Volpe, Nucl. Phys. A. **613**, 445 (1997).
[11] K. Hagino, S. Kuyucak, and N. Takigawa, Phys. Rev. C **57**, 1349 (1998).
[12] L. G. Gerchikov, C. Guet, and A. N. Ipatov, Phys. Rev. A **66**, 053202 (2002).
[13] F. Catara, D. Gambacurta, M. Grasso, and M. Sambataro, Phys. Lett. A **349**, 345 (2006).
[14] C. Yannouleas, Phys. Rev. C **35**, 1159 (1987).
[15] S. Drozdz, S. Nishizaki, J. Speth, and J. Wambach, Phys. Rep. **197**, 1 (1990).
[16] G. Lauritsch and P. G. Reinhard, Nucl. Phys. A. **509**, 287 (1990).
[17] K. Takayanagi, K. Shimizu, and A. Arima, Nucl. Phys. A. **477**, 205 (1988).
[18] A. Mariano, F. Krmpotic, and A. F. R. de Toledo Piza, Phys. Rev. C **49**, 2824 (1994).
[19] D. Gambacurta, M. Grasso, F. Catara, and M. Sambataro, Phys. Rev. C **73**, 024319 (2006).
[20] W. Ekardt, Phys. Rev. B **31**, 6360 (1985); W. Ekardt, *ibid.* **32**, 1961 (1985).
[21] C. Guet and W. R. Johnson, Phys. Rev. B **45**, 11283 (1992).
[22] P. Papakonstantinou and R. Roth, Phys. Lett. B **671**, 356 (2009).
[23] M. Tohyama and P. Schuck, Eur. Phys. J. A **19**, 203 (2004).
[24] M. Tohyama and P. Schuck, Eur. Phys. J. A **19**, 215 (2004).
[25] M. Tohyama, S. Takahara, and P. Schuck, Eur. Phys. J. A **21**, 217 (2004).
[26] S. Takahara, M. Tohyama, and P. Schuck, Phys. Rev. C **70**, 057307 (2004).
[27] M. Tohyama, Phys. Rev. C **75**, 044310 (2007).
[28] M. Grasso and F. Catara, Phys. Rev. C **63**, 014317 (2000).
[29] D. J. Thouless, Nucl. Phys. **21**, 225 (1960).
[30] S. Adachi and E. Lipparini, Nucl. Phys. A. **489**, 445 (1988).
[31] J. Borggreen, P. Chowdhury, N. Kebaili, L. Lundsberg-Nielsen, K. Lutzenkirchen, M. B. Nielsen, J. Pedersen, and H. D. Rasmussen, Phys. Rev. B **48**, 17507 (1993).
[32] C. Yannouleas, F. Catara, and N. Van Giai, Phys. Rev. B **51**, 4569 (1995).
[33] G. Onida, L. Reining, R. W. Godby, R. Del Sole, and Wanda Andreoni, Phys. Rev. Lett. **75**, 818 (1995).
[34] V. M. Silkin, M. Quijada, R. Dez Muino, E. V. Chulkov, and P. M. Echenique, Surf. Sci. **601**, 4546 (2007).
[35] V. G. Soloviev, *Theory of Atomic Nuclei: Quasiparticles and Phonons* (Institute of Physics, Bristol, Philadelphia, 1992).
[36] C. A. Bertulani and V. Yu. Ponomarev, Phys. Rep. **321**, 139 (1999).
[37] G. Colò and P. F. Bortignon, Nucl. Phys. A. **696**, 427 (2001).
[38] D. J. Rowe, Phys. Rev. **175**, 1283 (1968).
[39] H. Lenske and J. Wambach, Phys. Lett. B **249**, 377 (1990).
[40] S. Adachi and S. Yoshida, Nucl. Phys. A. **306**, 53 (1978).
[41] J. Wambach, Rep. Prog. Phys. **51**, 989 (1988).
[42] D. Lacroix, S. Ayik, and P. Chomaz, Prog. Part. Nucl. Phys. **52**, 497 (2004).
[43] S. Ait-Tahar and D. M. Brink, Nucl. Phys. A. **560**, 765 (1993).
[44] J. Dukelsky, G. G. Dussel, J. G. Hirsch, and P. Schuck, Nucl. Phys. A. **714**, 63 (2003).
[45] J. G. Hirsch, O. Civitarese, and M. Reboiro, Phys. Rev. C **60**, 024309 (1999).
[46] D. Gambacurta and F. Catara, Phys. Rev. B **77**, 205434 (2008).
[47] J. Speth and J. Wambach, *Electric and Magnetic Giant Resonances in Nuclei* (World Scientific, Singapore, 1991).